

# Concentration Fields of Reactants and Products Species in a Reacting Vortex Ring

**Shin-Juh Chen and Werner J.A. Dahm**  
*Laboratory for Turbulence and Combustion (LTC)*  
*Department of Aerospace Engineering*  
*The University of Michigan*  
*Ann Arbor, MI 48109-2140*

**Joel A. Silver**  
*Southwest Sciences, Inc.*  
*1570 Pacheco Street, Suite E-11*  
*Santa Fe, NM 87505*

**Gretar Tryggvason**  
*Laboratory for Turbulence and Combustion (LTC)*  
*Department of Mechanical Engineering and Applied Mechanics*  
*The University of Michigan*  
*Ann Arbor, MI 48109-2121*

## Introduction

The proposed paper will present experimental and numerical results on the concentration fields of both reactants and products species in a reacting vortex ring that is generated from the interaction between a diffusion flame and a laminar vortex ring. Flame-vortex interactions are canonical configurations used to study the underlying processes occurring in complicated turbulent reacting flows. This type of configuration contains many of the fundamental aspects of the coupling between fluid dynamics and combustion that could be investigated with more controllable conditions than are possible under direct investigations of turbulent flames. The current configuration has been studied experimentally by Chen & Dahm (1997-1999) and Chen *et al.* (2000a and b) under microgravity conditions, and by Park & Shin (1997), and You *et al.* (1998) under normal gravity conditions. This configuration is similar to that used in the analyses of Karagozian & Manda (1986) and Manda & Karagozian (1988) of their 2-D vortex pair in which both fuel and entrained oxidizer are present. The vortex ring used in this study is generated by issuing methane into an air environment through the exit of an axisymmetric nozzle. The experiments were conducted under microgravity conditions in order to remove the undesirable effects of buoyancy that can affect both the flame structure and ring dynamics resulting in possibly asymmetric and non-repeatable interactions (Chen & Dahm, 1997).

The experimental technique of diode laser wavelength modulation spectroscopy (WMS) is used to measure concentration fields of reactants, CH<sub>4</sub> and O<sub>2</sub>, products, H<sub>2</sub>O, CO<sub>2</sub>, OH, and temperature fields which can be inferred from either line pairs of O<sub>2</sub> or OH lines. This technique has been

investigated previously by Silver (1992) and Bomse *et al.* (1992). This is the first time that the technique is been applied to reacting vortex rings under microgravity conditions. The effect of ring circulation and fuel volume on the species concentration fields will be investigated. The experimental results will be compared to the current numerical results, and used to validate the numerical studies. In addition, the existence of burned cores during the interactions will be determined, and the increase in reactant consumption with increased ring circulation will be examined.

Numerical studies were also conducted by solving the Navier-Stokes and mixture fraction equations with the assumptions of unity Lewis and Schmidt numbers. Equilibrium chemistry and flamelet libraries were used to obtain the temperature and species mass fraction fields. The numerical results will serve as guidelines in conducting the experimental studies. Ring circulation and fuel volume effects on the interactions and species concentration fields will be investigated and compared to experimental results.

## Experimental Technique and Results

A photograph of the laser diagnostic layout is shown in Fig. 1 for the calibration sequence. This system is been incorporated into an existing drop rig that have been used to study diffusion flame-vortex ring interactions under microgravity conditions by Chen & Dahm (1997-1999) and Chen *et al.* (2000*a*, and *b*). The laser beam is collimated by an anti-reflection coated aspheric lens and is pointed onto a raster scanner mirror. As the mirror is rotated over an angle of about 30°, the reflected laser beam hits an off-axis paraboloidal reflector (OAP). The scanner mirror is positioned at the focus of this OAP so that all rays reflected by the OAP are parallel. As the beam is swept by the scanner, it tracks in parallel lines across the flame. After traversing the flame, a second off-axis paraboloid collects the beam and refocuses it onto a single photodetector. This optical system can scan a range of up to 4 cm. The result of this process is that data acquired sequentially in time are used to obtain spatially-resolved line-of-sight measurements across the flame. More details on this approach can be found in Silver & Kane (1999).

WMS detection is accomplished by digitally modulating the laser wavelength at 25 kHz and detecting the  $2f$  (50 kHz) component of the photocurrent. A modified square wave modulation waveform is used (Iguchi, 1986). Data are recorded using the analog inputs to a stand-alone digital signal processor (DSP) supercontroller. This device generates the scanner and laser ramp/modulation waveforms, acquires and processes all data, and stores the data to memory for subsequent download to a laptop computer after the drop is completed. The DSP board is housed in a small electronics box mounted on the drop rig. This box also contains the laser and scanner controllers, and the necessary cable interfaces.

This system is anticipated to detect methane, water, carbon dioxide, hydroxyl radicals and molecular oxygen. For the detection of oxygen at 760 nm (visible), a GaAlAs vertical cavity surface emitting laser is used. The other gases are detected using near-infrared InGaAsP distributed feedback lasers at the specific wavelengths required for each gas.

The procedure for data acquisition and analysis is as follows. Before the drop the system stores data in a circular buffer, so as to have pre-drop spectra if necessary and to aid in setting up the

served scalar equations are discretized using a Quadratic Upwind Interpolation for Convective Kinematics (QUICK) scheme. The viscous and diffusion terms are discretized using an implicit Crank-Nicholson scheme with centered differencing. Time integration was performed using a first-order scheme. Viscosity is taken to vary with temperature to the 0.7th power, and mass diffusion varies with temperature to the 1.7th power. Equilibrium chemistry and flamelet libraries were obtained from CET93 and OPDDIF.

Figure 3 shows the time evolution of  $\text{CH}_4$  mole fraction with ring circulation of  $100 \text{ cm}^2/\text{sec}$  and fuel volume of 21 cc. Fuel was injected at  $14.96 \text{ cm/s}$  for a period of 0.4468 sec. Strong rollup which resulted in the formation of vortex cores containing fuel is not observed here, but was seen in the case of similar ring circulation with fuel volume of 10.5 cc. With no surprise, the fuel concentration decreases inside the vortex as the fuel is been consumed by the reaction.

The  $\text{O}_2$  mole fraction contours are shown in Fig. 4. There is no presence of oxygen inside the vortex ring. Stoichiometric proportions of  $\text{O}_2$  diffuses into the ring and reacts with  $\text{CH}_4$  to form products inside the vortex ring. The numerical result strongly suggests that a diffusion-limited reaction is a very good approximation for estimating the fuel consumption time for the range of hydrodynamic parameters investigated here.

Temperature contours are shown in Figs. 5 with hot region marked by red and the ambient temperature region marked by blue. There are no hot regions inside the vortex rings. Cold regions inside the vortex rings are observed throughout the fuel injection period. This is not surprising since fuel at ambient temperature is been injected into an air environment which is also at ambient temperature (300 K). In the later stage of interaction, heat slowly diffuses into the vortex ring from the hot reaction zones; this is depicted by the slow disappearance of the blue regions inside the ring.

The time evolution of the  $\text{H}_2\text{O}$  fields are shown in Fig. 6, and the high concentration of water coincides with the regions of high temperature (as shown in Fig. 5). In addition, water concentrations are found on either side of the high temperature zones of the reacting vortex rings. Immediately after the fuel injection is shut-off, water generated in the flame zones continuously diffuse into the vortex ring. A thin blue region can be seen in the figures which separates the flame zone and the fuel zone.

However,  $\text{CO}_2$  concentration fields of Fig. 7 evolved very differently than the previous  $\text{H}_2\text{O}$  fields. Carbon dioxide concentration are only present near the high temperature zones, and exist only in thin regions near the flame. More precisely, the high concentration of  $\text{CO}_2$  lies toward the oxidizer side and does not overlap with the region of high temperature. Furthermore, no  $\text{CO}_2$  concentration is found inside the vortex ring where fuel is still present.

The full paper will discuss in details the effects of fuel volume and ring circulation on the species concentration fields of reacting vortex rings. Numerical results will also be compared to the experimental results for a wide range of hydrodynamic parameters.

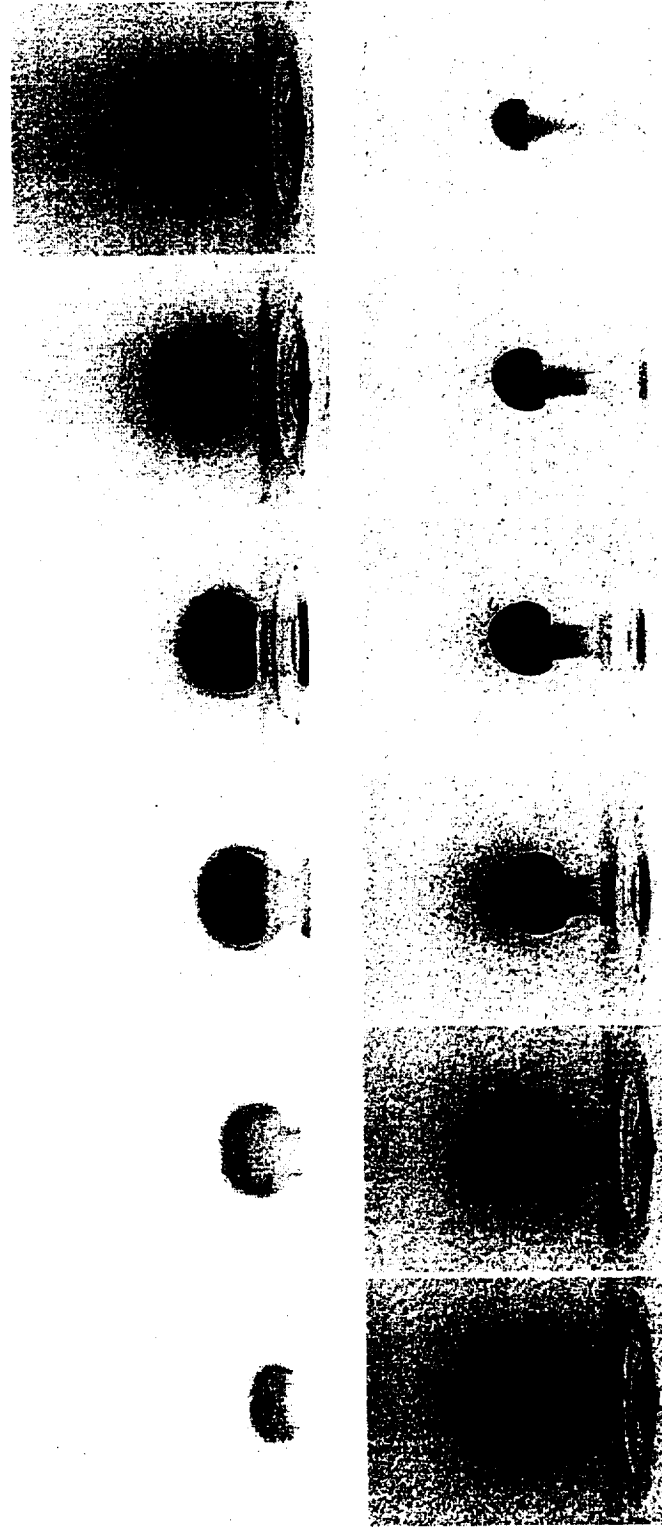


**Figure 2:** Propane-air combustion for ring circulation of  $150 \text{ cm}^2/\text{sec}$  and fuel volume of 9 cc. Frame rate is 30 fps from left to right. A reacting vortex ring emerges from the nozzle and forms a luminous bubble. The late stage of interaction is suggestive of a diffusion-limited reaction of the rich section of the vortex ring.

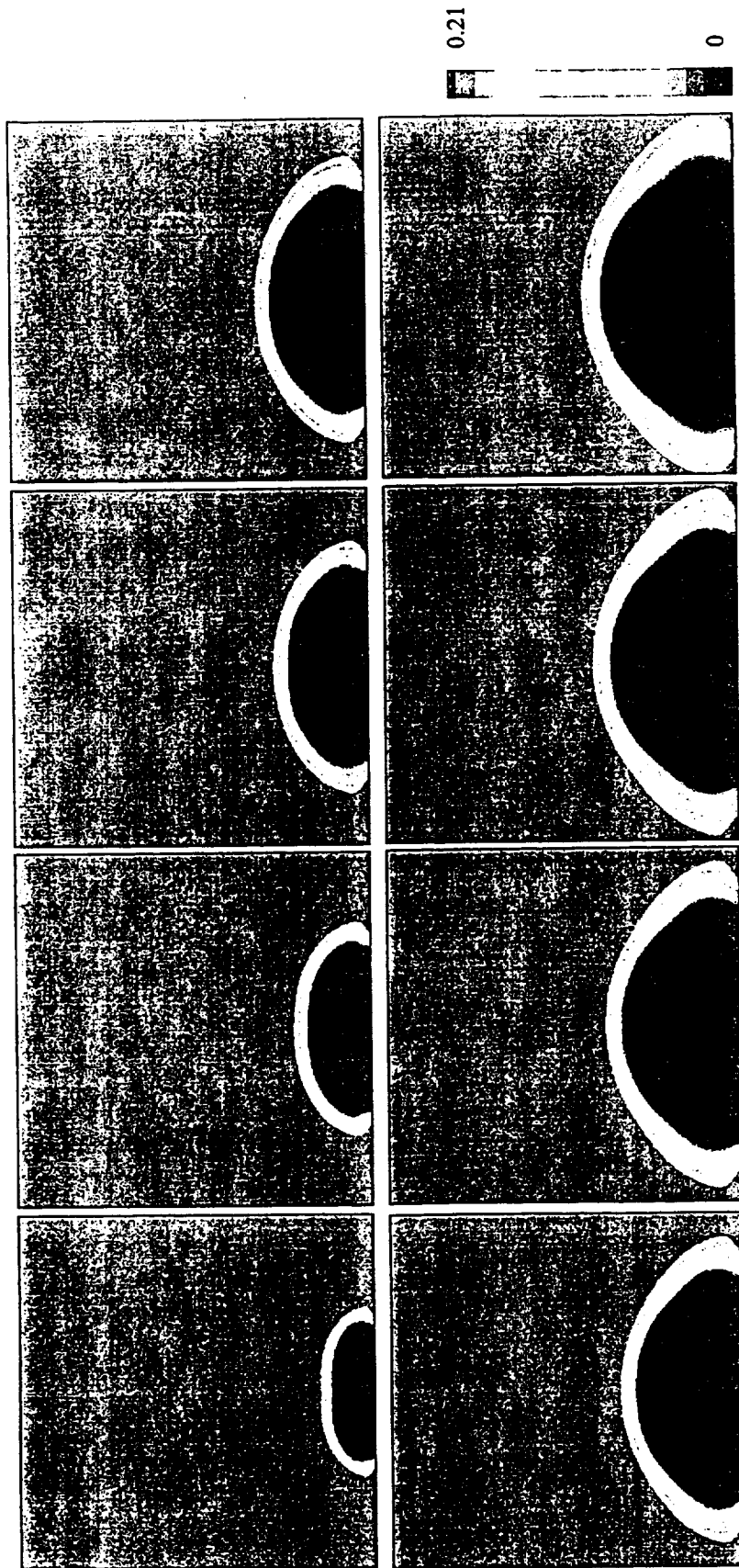
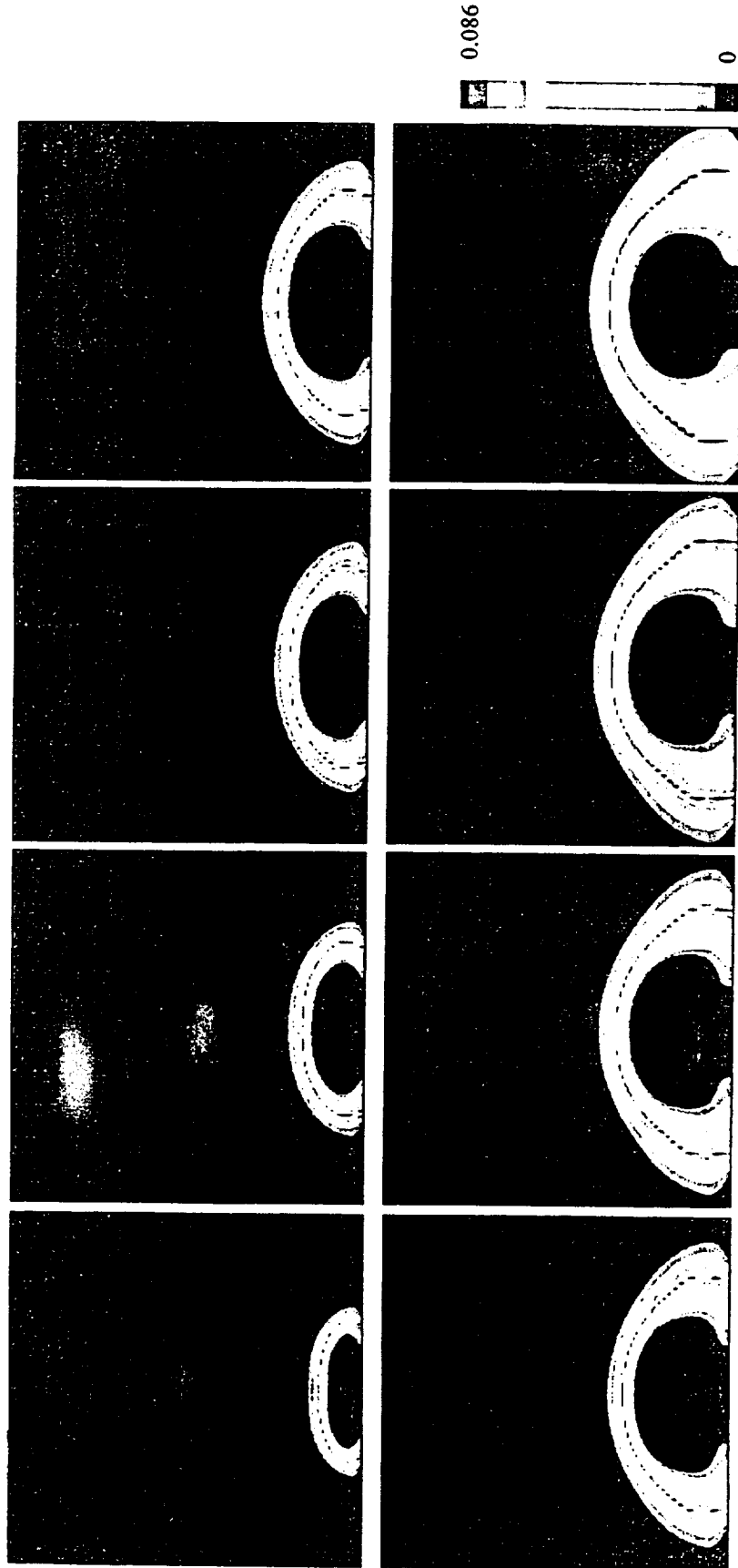


Figure 4: Simulation results showing the time evolution of  $O_2$  mole fraction for a reacting vortex ring. Ring circulation is  $100 \text{ cm}^2/\text{sec}$  and injected fuel volume is 21 cc. Methane is issuing into air environment. Time between frames is 0.100 sec.



**Figure 7:** Simulation results showing the time evolution of  $\text{CO}_2$  mole fraction for a reacting vortex ring. Ring circulation is  $100 \text{ cm}^2/\text{sec}$  and injected fuel volume is 21 cc. Methane is issuing into air environment. Time between frames is 0.100 sec.